Fourier domain mode locking at 1050 nm for ultra-high-speed optical coherence tomography of the human retina at 236,000 axial scans per second

R. Huber,[1,2,*] D. C. Adler,[1] V. J. Srinivasan,[1] and J. G. Fujimoto[1,*]

[1]*Department of Electrical Engineering and Computer Science and Research Laboratory of Electronics, Massachusetts Institute of Technology, Cambridge, Massachusetts 02139, USA*
[2]*Lehrstuhl für BioMolekulare Optik, Ludwig Maximilians Universität München, Fakultät für Physik, Oettingenstrasse 67, 80538 München, Germany*
**Corresponding authors: jgfuji@mit.edu; Robert.Huber@Physik.Uni-Muenchen.de*

Received March 21, 2007; accepted May 1, 2007;
posted May 23, 2007 (Doc. ID 81337); published July 10, 2007

A Fourier domain mode-locked (FDML) laser at 1050 nm for ultra-high-speed optical coherence tomography (OCT) imaging of the human retina is demonstrated. Achievable performance, physical limitations, design rules, and scaling principles for FDML operation and component choice in this wavelength range are discussed. The fiber-based FDML laser operates at a sweep rate of 236 kHz over a 63 nm tuning range, with 7 mW average output power. Ultra-high-speed retinal imaging is demonstrated at 236,000 axial scans per second. This represents a speed improvement of ~10× over typical high-speed OCT systems, paving the way for densely sampled volumetric data sets and new imaging protocols. © 2007 Optical Society of America

OCIS codes: 110.4500, 140.3600, 170.3880.

Optical coherence tomography (OCT) [1] is a high-resolution optical imaging technique with many biomedical applications. The largest clinical application of OCT is ophthalmology, where OCT can visualize cross-sectional structure of retinal pathologies [2]. For ophthalmic applications, high-speed OCT systems typically use a broadband light source in combination with a spectrometer [3,4] (spectral–Fourier domain OCT), which can achieve axial scan rates of several tens of kilohertz [5–7] and a maximum ranging depth of ~2 mm [5,8,9]. However, these acquisition speeds are still insufficient to acquire a densely sampled 3D data set *in vivo*. In ophthalmic OCT applications, the practical measurement time is limited to approximately 1 s, due to patient eye motion and blinking. An axial scan rate of ~250 kHz is therefore required to acquire a 512 frames × 512 axial scan data set, which is approximately 10× faster than what is possible with current high-speed systems.

The goal of increasing OCT imaging speed has been addressed using rapidly wavelength-swept lasers. Here the spectrometer is replaced by a high-speed photoreceiver. Previously, the maximum achievable axial scan rate, equivalent to the laser sweep repetition rate, was limited to several tens of kilohertz, due to fundamental speed limitations of conventional swept lasers [10,11]. Fourier domain mode locking (FDML) has been demonstrated to virtually remove these speed constraints [12]. In the 1300 nm wavelength range, sweep repetition rates of up to 370 kHz have been reported [13,14]. Wavelengths in the water absorption window from 1020–1120 nm are required for retinal imaging [15,16], where swept-source–Fourier domain OCT has been demonstrated at a speed of 18.8 kHz [17]. In this Letter, we present a detailed analysis of an FDML laser in the 1050 nm wavelength region, demonstrate a sweep repetition rate of 236 kHz, and use this laser for 3D *in vivo* ophthalmic imaging.

In an FDML laser, a narrowband optical bandpass filter is tuned with a period equal to a harmonic of the optical cavity round-trip time. The entire optical sweep is stored inside the cavity and it is not necessary to build up lasing from amplified spontaneous emission repeatedly [12]. The first implementations of FDML lasers were demonstrated at 1300 nm near the zero dispersion point of standard optical fiber [12,13]. In this wavelength range all optical frequency components have very similar cavity round-trip times and match one fixed filter tuning period. A first FDML criterion [12] is given by the synchronization condition $f_{drive}=c/(nl_{fiber})$, where l_{fiber} is the fiber length, c is the speed of light, and n is the refractive index of the fiber. However, for an operating wavelength of 1050 nm, there is linear dispersion in the optical fiber. The time delay per round-trip $\Delta\tau_{mismatch}$ between the longest and shortest wavelengths in the laser spectrum is $\Delta\tau_{mismatch}=l_{fiber}d\Delta\lambda_{tuning\ range}$, where d is the chromatic dispersion coefficient of the fiber, and $\Delta\lambda_{tuning\ range}$ is the total tuning bandwidth. For FDML operation, this time mismatch must be smaller than the time duration τ_{gate}, during which the bandpass filter transmits a single wavelength [12]. With the filter bandwidth $\Delta\lambda$, the filter drive frequency f_{drive}, and a factor $\eta=1/\pi$ accounts for the higher sweep speed in a bidirectional, sinusoidal sweep [10], the gate time τ_{gate} can be calculated as

0146-9592/07/142049-3/$15.00

$$\tau_{gate} = \frac{\eta \Delta\lambda}{f_{drive} \Delta\lambda_{tuning\ range}}. \quad (1)$$

Using the prerequisite $\tau_{mismatch} \leq \tau_{gate}$, we derive the second FDML criterion:

$$l_{fiber} d \Delta\lambda_{tuning\ range} \leq \frac{\eta \Delta\lambda}{f_{drive} \Delta\lambda_{tuning\ range}}. \quad (2)$$

Equation (2) can be solved for the filter bandwidth $\Delta\lambda$ as

$$\Delta\lambda \geq \frac{c \Delta\lambda^2_{tuning\ range} d}{\eta n}. \quad (3)$$

Equation (3) provides several interesting insights for FDML operation with a dispersive cavity. First, it is remarkable that, in a first approximation, the minimum filter bandwidth required for synchronization is independent of the cavity length. A longer cavity causes more dispersion and a larger temporal walk-off. However, the gating time τ_{gate} of the filter is also longer, which compensates for this effect. Secondly, the tuning range occurs as a quadratic factor in Eq. (3). This implies a large effect on the filter bandwidth requirements, when improved axial resolution is desired for OCT applications. It is important to emphasize that synchronization for only two optical round-trips/filter passes was assumed in this analysis. For improved operation, more round-trips and a longer effective cavity photon lifetime might be desired, which is provided by increasing the optical filter width. The following experimental results show the benefits and trade-offs for different filter bandwidths. Using the values $d \approx 40$ ps/nm/km and $n = 1.46$, a total filter tuning range of 80 nm, and $c = 3 \times 10^5$ km/s, a minimum filter bandwidth of 0.16 nm is estimated. Experimentally, FDML operation with a sweep range of over 60 nm was observed using fiber Fabry–Perot tunable filters (FFP-TFs) with bandwidths of 0.08, ~0.15, and ~0.3 nm. A comparison of FDML performance using these filters is described below.

Figure 1(A) shows the setup for the 1050 nm FDML laser. This is an "externally buffered" configuration, providing unidirectional sweeping at twice the filter drive frequency. This is similar to one previously presented [13], however, here the optical delay is outside the laser cavity. The cavity is a ring geometry with a total optical path length of 2.5 km. The gain medium is a semiconductor optical amplifier (SOA, Covega Corp.). An FFP-TF (0.15 or 0.3 nm from LambdaQuest, Inc. and 0.08 nm from Micron Optics, Inc.) driven at 118 kHz is used for tuning and is driven synchronously to the cavity round-trip frequency of 118.352 kHz. A 523 m length of fiber in an external Mach–Zehnder interferometer provides a 2.55 μs delay before the light is combined with a 50/50 coupler and postamplified by a booster SOA (QPhotonics, LLC) with a slightly blueshifted gain to improve spectral shape [10]. Retinal imaging is performed using a pair of galvanometer scanning mirrors and relay optics [18]. The FDML laser is operated with the 0.3 nm FFP-TF (LambdaQuest, Inc.). The average power on the cornea is 1.4 mW. The data acquisition system for imaging and source characterization is described previously [12,13].

Figure 1(B) shows the output spectrum of the FDML laser. The spectrum is centered at ~1070 nm, which corresponds to the water absorption minimum [15,16]. The average output power is ~7 mW after the booster SOA. The full width is 63 nm (FWHM 38 nm), which corresponds to a maximum OCT axial resolution of 15 μm in air and 11 μm in tissue. Figure 1(C) shows the fringe traces from a single reflection in the sample arm. Two sweeps, each 2.55 μs in duration, are followed by a 3.35 μs delay. This delay is necessary for the analog-to-digital converter to rearm the trigger. One trigger starts the acquisition for one pair of sweeps ($2 \times 512 = 1024$ samples), so that two axial scans are acquired with one trigger event. Figure 2 shows the point-spread functions (PSF) for isolated reflections at different image depths for FFP-TFs with different bandwidths. It can be seen that the 0.08 and 0.15 nm filters show comparable roll off at short delays (~6 dB over 1.75 mm in air), whereas a 0.3 nm filter leads to a faster roll off (~6 dB over 1.2 mm). At longer delays, the PSF roll off for the

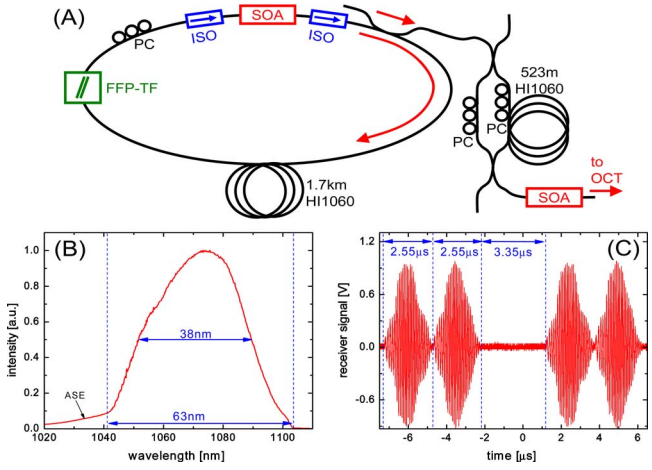

Fig. 1. (Color online) (A) Setup of the buffered FDML laser. (B) Output spectrum of the laser. (C) Transient fringe traces from interferometer.

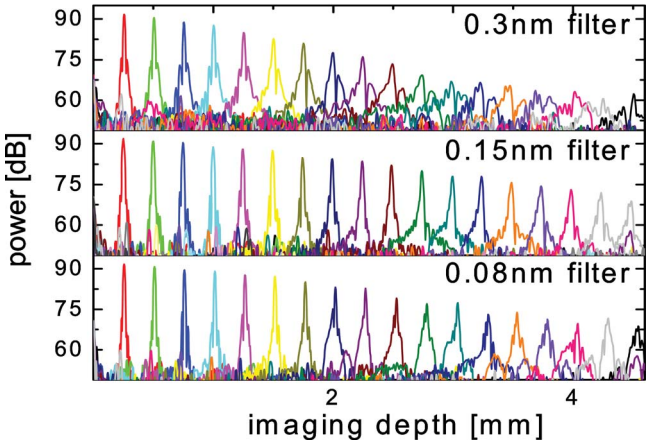

Fig. 2. (Color online) PSF in air for different delays and filter bandwidths. The y axis is normalized to show system sensitivity.

0.15 nm filter is slightly better than for the 0.08 nm filter. This could be due to the increased loss of light after one round-trip in the case of the 0.08 nm filter, caused by the cavity dispersion. This observation supports the estimation of the optimum filter width of ~0.16 nm. The maximum measured sensitivity at short delays is ~91 dB for both sweep directions, while the theoretical shot-noise limit is 99 dB. One can attribute 5.5 dB of the sensitivity penalty to backcoupling losses in the sample arm; the remaining 2.5 dB can be attributed to relative intensity noise and phase noise caused by the amplified spontaneous emission background. The measured resolution is ~19 μm in air and 13.7 μm in tissue for all filters and is almost independent on the imaging depth over more than 2 mm (~1.5 mm for the 0.3 nm filter). The degradation in axial resolution compared to the theoretically predicted 15 μm can be attributed to the process of numerical spectral shaping and apodization. Figure 3 shows the application of the FDML laser for *in vivo* retinal imaging. The *en face* image in Fig. 3(A) shows a fundus view reconstructed by axially summing a data set of 512 pixels × 512 axial scans × 400 frames, acquired in 0.86 s. No transverse motion artifacts are visible. Figure 3(B) shows an oblique view of a 3D reconstruction. Figure 3(C) shows a cross-sectional image consisting of 8192 axial scans acquired in 34 ms.

In conclusion, an FDML laser operating at a new wavelength in a nonzero dispersion regime is discussed, design rules are derived, and operation at 1050 nm without additional dispersion compensating elements is presented. Retinal OCT imaging at a speed of 236,000 axial scans per second is demonstrated. These results suggest that swept-source/Fourier-domain OCT can outperform current ophthalmic OCT systems by 1 order of magnitude in speed. The high speed will enable new imaging protocols and promises to make clinical *in vivo* 3D retinal topology mapping without motion artifacts feasible. Further improvements in bandwidth, axial resolution, speed, and image quality can be expected in the future.

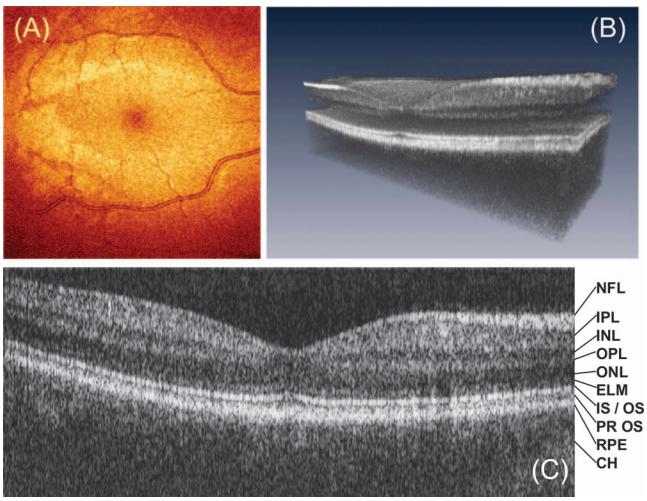

Fig. 3. (A) *En face* fundus view of retina generated from a 3D data set consisting of 512 lines × 400 frames. (B) Three-dimensional cut away reconstruction. (C) Cross-sectional image. NFL, nerve fiber layer; GCL, ganglion cell layer; IPL, inner plexiform layer; INL, inner nuclear layer; OPL, outer plexiform layer; ONL, outer nuclear layer; ELM, external limiting membrane; IS/OS, photoreceptor inner segment/outer segment junction; PR OS, photoreceptor outer segments; RPE, retinal pigment epithelium; CH, choroid.

This research was sponsored by the National Science Foundation (grant BES-0522845), National Institutes of Health (grants R01-EY011289-20 and CA75289-09), Air Force Office of Scientific Research (grants FA9550-040-1-0046 and FA9550-040-1-0011), and Natural Sciences and Engineering Research Council (NSERC) (Canada). J. G. Fujimoto receives royalties from intellectual property owned by MIT and licensed to Carl Zeiss Meditec.

References

1. D. Huang, E. A. Swanson, C. P. Lin, J. S. Schuman, W. G. Stinson, W. Chang, M. R. Hee, T. Flotte, K. Gregory, C. A. Puliafito, and J. G. Fujimoto, Science **254**, 1178 (1991).
2. C. A. Puliafito, M. R. Hee, C. P. Lin, E. Reichel, J. S. Schuman, J. S. Duker, J. A. Izatt, E. A. Swanson, and J. G. Fujimoto, Ophthalmology **102**, 217 (1995).
3. A. F. Fercher, C. K. Hitzenberger, G. Kamp, and S. Y. Elzaiat, Opt. Commun. **117**, 43 (1995).
4. G. Häusler and M. W. Lindner, J. Biomed. Opt. **3**, 21 (1998).
5. R. Leitgeb, C. K. Hitzenberger, and A. F. Fercher, Opt. Express **11**, 889 (2003).
6. J. F. de Boer, B. Cense, B. H. Park, M. C. Pierce, G. J. Tearney, and B. E. Bouma, Opt. Lett. **28**, 2067 (2003).
7. M. A. Choma, M. V. Sarunic, C. H. Yang, and J. A. Izatt, Opt. Express **11**, 2183 (2003).
8. N. A. Nassif, B. Cense, B. H. Park, M. C. Pierce, S. H. Yun, B. E. Bouma, G. J. Tearney, T. C. Chen, and J. F. de Boer, Opt. Express **12**, 367 (2004).
9. M. Wojtkowski, V. J. Srinivasan, T. H. Ko, J. G. Fujimoto, A. Kowalczyk, and J. S. Duker, Opt. Express **12**, 2404 (2004).
10. R. Huber, M. Wojtkowski, K. Taira, J. G. Fujimoto, and K. Hsu, Opt. Express **13**, 3513 (2005).
11. A. Bilenca, S. H. Yun, G. J. Tearney, and B. E. Bouma, Opt. Lett. **31**, 760 (2006).
12. R. Huber, M. Wojtkowski, and J. G. Fujimoto, Opt. Express **14**, 3225 (2006).
13. R. Huber, D. C. Adler, and J. G. Fujimoto, Opt. Lett. **31**, 2975 (2006).
14. D. C. Adler, R. Huber, and J. G. Fujimoto, Opt. Lett. **32**, 626 (2007).
15. K. F. Palmer and D. Williams, J. Opt. Soc. Am. **64**, 1107 (1974).
16. A. Unterhuber, B. Povazay, B. Hermann, H. Sattmann, A. Chavez-Pirson, and W. Drexler, Opt. Express **13**, 3252 (2005).
17. E. C. W. Lee, J. F. de Boer, M. Mujat, H. Lim, and S. H. Yun, Opt. Express **14**, 4403 (2006).
18. V. J. Srinivasan, R. Huber, I. Gorczynska, J. G. Fujimoto, J. Y. Jiang, P. Reisen, and A. E. Cable, Opt. Lett. **32**, 361 (2007).